Mredha et al. *NPG Asia Materials* (2023) 15:22
https://doi.org/10.1038/s41427-023-00472-1

NPG Asia Materials

ARTICLE Open Access

Tardigrade-inspired extremotolerant glycerogels

Md. Tariful Islam Mredha[1], Yoonseong Lee[1], Adith Varma Rama Varma[1], Tanish Gupta[1], Rumesh Rangana Manimel Wadu[1] and Insu Jeon[1]

Abstract

We developed extremotolerant glycerogels (GGs) with well-modulated polymer structures, functions, and properties, inspired by the tun formation of tardigrades. GGs comprising extreme protected intra- and intermolecular networks are obtained through a very slow structure building process, which includes the smooth replacement of water in predesigned hydrogels with glycerol and thermal annealing while retaining the structures and functions of the original hydrogels. Four different GGs are fabricated as proofs-of-concept using different crosslinkers and polymers. Although various polyol-based wide-temperature-tolerant gels fabricated by conventional methods fail to demonstrate stabilities at low and high temperature extremes simultaneously, the GGs fabricated by our bioinspired method exhibit long-term stability (approaching one month) over an extremely wide temperature range (−50–80 °C) and thermal-shock-absorption capabilities at 150 °C. Furthermore, our versatile method enables us to program GGs with wide ranges of stiffness, strength, stretchability, and toughness values and elasticity, plasticity, hysteresis, and self-recoverability capabilities. The self-weldability, electrical patternability, and applicability characteristics of the GGs as electrolytes and supercapacitors demonstrate their complex 3D designability and facile functionalization capability aspects. The various functional GGs developed through the proposed method are applicable for the design of diverse extremotolerant, flexible, and stretchable devices for biological, electrical/electronic, and soft robotics applications.

Introduction

Gels, which are a class of semisolid materials formed by crosslinked 3D polymer networks swollen in specific solvents, have attracted significant attention due to their applications in biomedicine, flexible electronics, energy-storage devices, sensors/actuators, and soft robotics. Gels exhibit a wide variety of functions, including electrical, thermal, actuation, shape-morphing, stimuli-responsive, and biomimetic properties that no other solid or liquid material exhibit alone[1–6]. Hydrogels are formed by water-swollen hydrophilic polymer networks and are widely used due to their biocompatibility and immense scope for biomedical applications[1–3,7–11]. Although many strategies have been developed for designing hydrogels with various functionalities, their applications have been mainly confined to aqueous environments. Moreover, the short lifetime in air limits the majority of the applications of hydrogels in nonaqueous environments, particularly under harsh environmental conditions, such as subzero and high temperatures[1,6,12,13].

Recently, several methods have been developed for improving the stabilities of gels under extreme environments. For example, double-hydrophobic-coated hydrogels have long-term air stabilities[12]. Ionic liquid-based ionogels exhibit wide temperature tolerance levels[14,15]. However, ionic liquids are generally expensive, and many of them are harmful to the environment[16], making them less suitable for mass applications. The mechanical properties of ionogels depend strongly on polymer–solvent interactions; therefore, despite the wide temperature stabilities of ionic liquids, the mechanical properties of ionogels vary significantly with changes in temperature due to variations in the polymer–solvent interactions[14,15]. In recent years, biofriendly and inexpensive polyol solvents, such as glycerol, propylene glycol, and ethylene glycol, that exhibit wide-temperature stability have attracted significant attention for the

Correspondence: Insu Jeon (i_jeon@chonnam.ac.kr)
[1]School of Mechanical Engineering, Chonnam National University, 77 Yongbong-ro, Buk-gu, Gwangju 61186, Republic of Korea

development of extremotolerant gels[11,13,14,17–27]. Myriad glycol/water-based organohydrogels reportedly possess good antifreezing capabilities at subzero temperatures[13,14,17–27]. Photoresponsive gels based on metal coordination bonding have been developed from glycerol/water mixtures; these gels are functional at subzero temperatures[17]. A gel fabricated from an ethylene glycol/water mixture has good negative-temperature ionic conductivity[18]. Although a glycol/water mixture induces good antifreezing performance, it eliminates the antiheating capabilities of the gels. A few reports have overstated the antiheating capabilities, as is evident below. For instance, the examination of properties through quick thermal scanning or after a short storage period (≤1 d) has revealed the high stabilities of glycol/water-based gels at elevated temperatures[17–19,23,24]. However, most of the water from the gel network is lost within 1 d, even at room temperature (25 °C)[23,24]. To induce antiheating capabilities, pure glycol-based gels have been fabricated[6,24–27]. However, none of the aforementioned gel materials exhibit durable performance characteristics at extremely cold (<−30 °C) and hot (>60 °C) temperatures simultaneously.

Most of the glycol-based gels are fabricated directly in glycol-based solvents or the water of the prefabricated hydrogels substituted with organic solvents. The direct fabrication of gels in pure glycol-based solvents with good structural integrity is difficult because the high viscosities of the solvents and the polymerization-induced phase separation decrease the degree of polymerization, thereby hindering 3D gel-structure formation[24]. Hence, water/glycol-based mixed solvents are used for direct gel fabrication at the expense of the antiheating capability[13,17–19,21,22,24,26]. Substituting the solvent of prefabricated hydrogels with a viscous organic solvent leads to undesired phase separation and polymer aggregation because the high osmotic pressures of viscous solvents or the alterations in polymer–solvent affinities markedly deswell the gel[28]. Therefore, both of these strategies induce undesirable structural changes, which limit the performance and durability levels of gels at extreme temperatures. To overcome these limitations, it is necessary to develop extremotolerant gels with crosslinking/toughening mechanisms and functionalities that are durable at extremely low and high temperatures. To this end, tardigrades are considered inspirational because they are the most resilient lifeforms on earth; they can survive under extreme conditions—at extremely low and high temperatures and pressures, in dry weather, and under intense radiation (Fig. 1a)[29–32]. Under harsh environmental conditions, tardigrades undergo structural transition to a form known as the tun state by slowly removing most of their nonbonded free water and simultaneously producing bioprotective molecules, such as sugars (including trehalose and glycerol) and proteins[30–32]. Slow dehydration is vital for extremotolerant tun formation[32] because this slow process allows the biosynthesized molecules to form intramolecular and intermolecular bonding networks with biomolecules and cells and to thereby prevent irreversible damage under harsh conditions. Inspired by the tun formation of tardigrades, a novel class of extremotolerant gel materials is designed using glycerol, preserving the polymeric structures, functions, and properties of gels under extreme conditions. Glycerol is a low-molecular-weight polyol, and it is bioderived, inexpensive, and applicable as a green solvent (Fig. 1b)[33]; it is rich in hydroxyl groups and forms an internal facile H-bonding network with various hydrophilic polymers[22,34–36]. Glycerol exhibits excellent supercooling to its glass transition temperature (−83 °C), extremely low vapor pressures (133.3 Pa at 125 °C) and extremely high boiling temperatures (290 °C)[35,37]. Pure glycerol is adopted as an extreme protectant molecule for the gel network because it exhibits functions similar to those of sugar and protein when protecting the tun state.

In this study, we propose a facile and versatile very slow two-step structure-forming process for fabricating various extremotolerant glycerogels (GGs) with various properties and functions. The complete process is termed very slow because the gel structure is fabricated very slowly through multiple steps. Furthermore, only simple physical methods are employed for converting the hydrogels into extreme tolerant glycerogels. Therefore, the process is termed facile. This method allows the use of numerous functional hydrogels[1–11] as base materials. While bioprotective molecules are biologically synthesized in tardigrades, we have supplied glycerol as a gel-protecting molecule by a simple diffusion-driven solvent-exchange process. In the first step, the water in the predesigned hydrogel network is replaced very slowly (stepwise manner within a span of 3 d) with glycerol by harnessing the high water–glycerol affinity due to H-bond formation. This slow solvent-exchange process allows glycerol to form an efficient intramolecular and intermolecular H-bonding network with polymer chains without significantly disrupting the structures and functions of the original hydrogels, mimicking the structural transitions of tardigrades (Fig. 1c). In contrast, direct solvent exchange causes notable gel shrinkage; upon immersing a typical water-equilibrated poly(vinyl alcohol) (PVA) hydrogel in glycerol, the gel removes most of its water and shrinks to a weight fraction (W) of 38% (Fig. 1c). The proposed bioinspired process prevents or significantly mitigates shrinkage-induced phase separation and polymer aggregation in water-equilibrated hydrogels by slowly replacing the water molecules and building a stable glycerol–polymer network. This strategy is implementable for various water-equilibrated hydrogels that usually

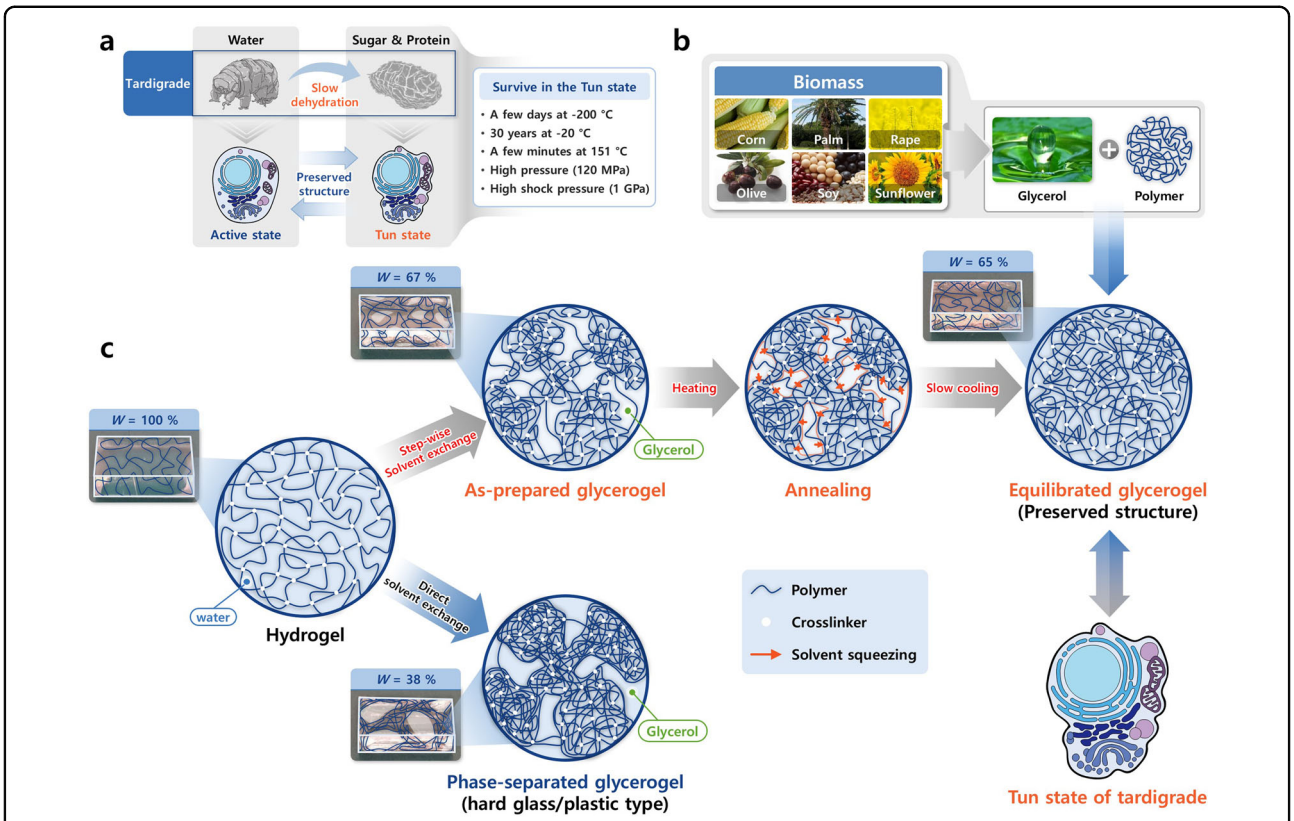

Fig. 1 Tardigrade-inspired strategy for designing extremotolerant GGs. a Tardigrades transform to the tun state under extreme conditions by preserving their integral structure because they withstand various harsh environmental conditions. **b** Inspired by the tun formation of tardigrades, extremotolerant multifunctional GGs are designed by integrating various polymers with glycerol, which is a biofriendly solvent[33]. **c** Initially, the water in the predesigned functional hydrogels is sequentially replaced with glycerol to minimize the damage to the integral structure of the gel. Thereafter, the as-prepared GG is dry-annealed to release undesired residual stresses and to obtain the final GG with a preserved polymer structure, mimicking tun formation in tardigrades. In contrast, direct solvent exchange results in a phase-separated hard structure inside the gel network.

undergo dramatic shrinkage by glycerol exchange. However, some hydrogels, such as polyacrylamide, swell significantly when water or water/glycerol mix solvents are used and become very weak in the equilibrated state; therefore, sequential solvent exchange should not be employed for these gels. For this class of high water-swelling hydrogels, we have rationally adopted a high-temperature-induced direct solvent exchange process in pure glycerol instead of stepwise exchange at room temperature, preventing the swelling of the polymers due to the rapid replacement of the majority of water from the gel network with glycerol, and it builds a stable glycerol–polymer network. Upon completion of solvent exchange, undesired residual stresses on the gel network are released by thermal annealing of the gel in the second step. The method is versatile, enabling the conversion of a wide variety of hydrogels to extremotolerant GGs with excellent functions and properties.

In general, the solvent-exchange strategy is not a new idea in materials science. Various types of solvent exchanges have been performed for fabricating different classes of functional gels[2,38,39]. Preservation of biochemical structure through the gradual replacement of solvent is known in the field of biology. However, particularly for polyol-based extremotolerant gels, the reported solvent-exchange strategies and other methods fail to demonstrate stability at extremely low and high temperatures simultaneously. Inspired by the tun-forming processes of tardigrades, for the first time, we realize that much of the structural preservation of original hydrogels is key for achieving extremotolerant polyol-based gels. Therefore, we propose a generalized and rational solvent-exchange strategy for various polymers and crosslinkers for fabricating polyol-based extremotolerant gels. Reliable materials that are useful under extreme environments dramatically enhance their application potential and protect humans, machines, and the planet[40]. High temperatures generated in cars, bullet trains and plane engines, accident-induced heat generation in electrical devices, high-speed friction in machines, and high-level radiation in nuclear plants are some examples of materials facing extreme environments on a daily basis. Gel-based

materials are inherently susceptible to extreme environments. However, the requirements of gel-based materials with tolerance to extreme environments are significantly increasing in the fields of bionics, bioelectronics, wearable devices, soft energy-storage devices, soft machines, and robotics. Therefore, the proposed idea of developing extremotolerant glycerogels is expected to open a new avenue in gel science and to significantly enhance the application potentials of gels in those fields.

Materials and methods

Materials and instrumentation

Acrylamide (AAm), acrylic acid (AAc), *N*,*N*′-methylene-*bis*-acrylamide (MBAA), dimethyl sulfoxide (DMSO), propylene glycol, and iron(III) chloride ($FeCl_3$) were purchased from Daejung Chemicals & Metals Co., Ltd. (Republic of Korea). Glycerol, ethylene glycol, *N*,*N*′-dimethylacetamide (DMAc), ethanol, and lithium chloride (LiCl) were purchased from Samchun Pure Chemical Co. Ltd. (Republic of Korea). Cellulose-based filter paper (ADVANTEC) was purchased from Toyo Roshi Kaisha Ltd. (Japan). Poly(vinyl alcohol) (M_w: 89,000–98,000), ammonium persulfate (APS), and lithium perchlorate ($LiClO_4$) were purchased from Sigma Aldrich. Tripropylene glycol was purchased from Acros Organics (Belgium). The carbon nanotube (CNT) film (thickness: 10–20 μm) was purchased from Chengdu Organic Chemicals Co., Ltd., Chinese Academy of Sciences (China). All chemicals were used directly without further purification. Ultrapure deionized water was used in the experiments as needed.

All mechanical tests were performed under ambient conditions (humidity: 30–60%; temperature: ~25 °C) using a TEST ONE TO-100-1C universal testing machine (Republic of Korea) equipped with a 10 kgf load cell. The thermal stability and glass transition temperature (T_g) values of various GGs were determined using a differential scanning calorimetry (DSC) system (DSC823e, Mettler Toledo, Switzerland). The structure of the gel was observed by scanning electron microscopy (SEM) (S-4700, Hitachi, Japan). Fourier transform infrared (FT–IR) spectra of GGs were recorded on a Spectrum 3 FT–IR Spectrometer (PerkinElmer, USA). All electrochemical measurements of the fabricated PVA GG electrolyte and supercapacitor—electrochemical impedance spectroscopy, cyclic voltammetry (CV), and galvanostatic charge/discharge (GCD) tests—were performed using a Metrohm Multi Autolab/M204 multichannel potentio-galvanostat (The Netherlands).

Fabrication of polyacrylamide (PAAm) GGs

Initially, the PAAm hydrogel was prepared via free-radical polymerization in the following manner. A precursor solution containing 3 M of the AAm monomer, 0.05 mol% (with respect to monomer concentration) of the MBAA crosslinker, and 0.1 mol% (with respect to monomer concentration) of the APS initiator was prepared using deionized water. The solution was poured into a rectangular mold that was prepared by sandwiching a silicone rubber gasket of 3 mm thickness between two flat plastic plates. Thereafter, polymerization was performed by incubating the mold at 60 °C for 8 h. The as-prepared PAAm hydrogel was removed from the mold and immersed in preincubated glycerol at 60 °C for 2 h to allow for the maximum exchange of water with glycerol without any swelling in the PAAm gel. Thereafter, the gel was immersed in glycerol for 3 d at 25 °C to ensure the complete exchange of water with glycerol. The as-prepared GG was dry annealed in a closed glass vial at 100 °C for 3 h and then slowly cooled to 25 °C to obtain the desired PAAm GG (thickness ≈ 2.6 mm), which was used for further characterization.

Fabrication of PVA GGs

Initially, the PVA hydrogel was prepared by freeze–thawing, as described in a previous study[7] with slight modifications. A PVA solution was prepared by dissolving PVA powder in a DMSO/water (75:25, w/w) mixture under continuous stirring at 140 °C overnight. The DMSO/water mixture would produce fine crystals of PVA chains at subzero temperatures[41]. Unless otherwise noted, a 10 wt.% PVA precursor solution was used to fabricate the original PVA GG. The solution was inserted into a rectangular plastic mold of 3 mm thickness (prepared by sandwiching a silicone rubber gasket between two plastic plates). Thereafter, the mold containing the polymer solution was incubated at −50 °C for 1 d, which was followed by thawing at 25 °C for 12 h. The gel that formed was removed from the mold and immersed in water for 3 d. The water was replaced repeatedly to obtain a water-equilibrated PVA hydrogel. This gel was immersed sequentially in aqueous solutions of 25%, 50%, 75%, and 100% glycerol for 12, 12, 24, and 24 h, respectively, to obtain PVA GG. The as-prepared GG was annealed in a closed glass vial at 120 °C for 6 h and then slowly cooled to 25 °C to obtain the desired PVA GG (thickness ≈ 1.8 mm), which was used for further characterization.

Fabrication of poly(acrylamide-*co*-acrylic acid)/iron(III) (P(AAm-*co*-AAc)/Fe^{3+}) GGs

Initially, a P(AAm-*co*-AAc) hydrogel was prepared by the free-radical copolymerization of AAm and AAc. A precursor solution containing 3 M AAm and 0.6 M AAc in the presence of 0.1 mol% MBAA and 0.1 mol% APS (with respect to the total quantity of monomers) as the crosslinker and initiator, respectively, was prepared in water. The solution was inserted into a plastic mold (prepared by sandwiching a silicone rubber gasket

between two plastic plates) of 2 mm thickness and polymerized at 60 °C for 8 h. The as-prepared (P(AAm-*co*-AAc)) hydrogel was removed from the mold and immersed in a 0.075 M aqueous $FeCl_3$ bath for 1 d for ion binding. Thereafter, the superfluous ion from the gel was removed by washing the gel in pure water for 1 d, and the desired water-equilibrated (P(AAm-*co*-AAc)/Fe^{3+}) hydrogel was obtained. Subsequently, the as-prepared GG was obtained by a sequential solvent-exchange process (0%→25%→50%→100%), similar to the process described for fabricating the PVA gel. The as-prepared GG was initially wet-annealed in a glycerol bath at 120 °C for 2 h and cooled slowly to 25 °C. The gel was subjected to closed dry annealing at 120 °C for 6 h and slowly cooled to 25 °C to obtain the desired P(AAm-*co*-AAc)/Fe^{3+} GG (thickness ≈ 1.6 mm), which was used for further characterization.

Fabrication of cellulose GGs

Initially, cellulose hydrogels were prepared using cellulose paper. Small pieces of cellulose filter paper were sequentially washed using water (~6 h), ethanol (~6 h), and DMAc (~12 h), after which they were vacuum-dried at 60 °C. A 1.5% (w/w) cellulose solution was prepared by dissolving cellulose paper in a DMAc/LiCl (92:8, w/w) solvent. The cellulose solution was cast into a flat glass mold with a depth of 3 mm and exposed to ambient conditions (temperature: ~25 °C and humidity: 30–60%) for ~3 d to induce the gelation of cellulose through H-bond formation. The as-prepared organogel was sequentially equilibrated in ethanol (1 d) and water (1 d) to obtain a cellulose hydrogel. The water in the hydrogel network was replaced with glycerol through a sequential solvent-exchange process (0%→25%→50%→100%) that was identical to the process described for fabricating the PVA gel. Subsequently, this gel was dry annealed in a closed glass vial at 120 °C for 6 h and finally cooled slowly to 25 °C to obtain cellulose GG (thickness ≈ 2 mm); it was used for further characterization.

Fabrication of patterned GGs

A predesigned fractal-shaped silver pattern was created on a PVA GG surface using the mask-induced ion-sputtering method. A soft PVA GG sheet (40 mm × 30 mm × 1.7 mm) fabricated from a 4 wt.% precursor solution was used. A commercial ion-sputtering machine (Magnetron sputtering system, ALPHAPLUS, Republic of Korea) was used for sputtering. The sample was covered with a predesigned mask and set on the sample holder, which was subsequently placed on the anode. Silver sputtering was performed under vacuum conditions (pressure: 1.33×10^{-4} N m^{-2}) with argon flow (flow rate: 20 cm^3 min^{-1}) for 4 min under the application of a direct current of 2 A. Thereafter, the sample was extracted from the chamber, and the mask was removed to obtain the desired silver-patterned GG.

Fabrication of the GG-based electrolyte and supercapacitor

The PVA-GG-based electrolyte was fabricated using $LiClO_4$ as the salt ion source. Initially, a soft PVA gel was fabricated from a 5 wt.% precursor solution in DMSO/water (75:25, w/w) using a plastic mold with a thickness of 0.5 mm. After freezing (−50 °C, 1 d) and thawing (25 °C, 12 h), the gel was equilibrated in water (3 d), and then sequentially equilibrated in 25% (12 h) and 50% (12 h) glycerol (w/w). Subsequently, the gel was equilibrated in a solution containing 20% $LiClO_4$ in 75% aqueous glycerol (w/w) for 1 d. Finally, the gel was equilibrated in a solution of 20% $LiClO_4$ in pure glycerol (w/w) for 1 d to obtain the as-prepared PVA GG electrolyte (thickness ≈ 0.2 mm). The gel electrolyte sheet was cut into squares with dimensions of 20 mm × 20 mm and sandwiched between two parallel CNT films (20 mm × 20 mm), which served as the anode and cathode. The sandwiched CNT electrodes and PVA GG-$LiClO_4$ electrolyte were annealed in a closed glass vial at 90 °C for 3 h and slowly cooled to 25 °C to obtain the desired PVA-GG-electrolyte-based flexible supercapacitor (CNT/PVA GG-$LiClO_4$).

Results and discussion

Extreme tolerance, mechanical properties, and structures of GGs

Four basic GGs with various crosslinking structures and properties have been fabricated as proofs-of-concept: PAAm GGs (using a covalent crosslinker); PVA GGs (using a H-bonded polymer); P(AAm-*co*-AAc)/Fe^{3+} GGs (using dual crosslinkers (covalent bonding and Fe^{3+}-coordination)); and cellulose GGs (using a H-bonded pure biopolymer) (Fig. 2). All GGs exhibit excellent long-term stability (~7 d) over −50–80 °C. Upon exposure to air at −50, 25, and 80 °C for 1 week, the weight changes of all gels remain within ±10 wt.% (Fig. 3a and b; Fig. S1). The small increases or decreases in weight are caused by the absorption of atmospheric moisture or the loss of glycerol from the gel network, respectively.

The natures and structures of the different polymers and crosslinkers facilitate the systematic fabrication of the different GGs exhibiting wide ranges of tunable mechanical performance levels (Fig. 3c–f; Fig. S2–S5). For example, the loosely crosslinked soft PAAm GG stretches at >1200% and exhibits a low modulus (0.09 ± 0.003 MPa) and strength (0.22 ± 0.02 MPa). The strong H bonding, semicrystalline nature, and excellent energy dissipation capability of PVA result in a PVA GG with a high stiffness (8.9 ± 0.2 MPa) and strength (8.5 ± 0.01 MPa) and an extremely high work of extension (49.9 ± 0.4 MJ m^{-3}). The dual-crosslinked P(AAm-*co*-AAc)/Fe^{3+} GG exhibits

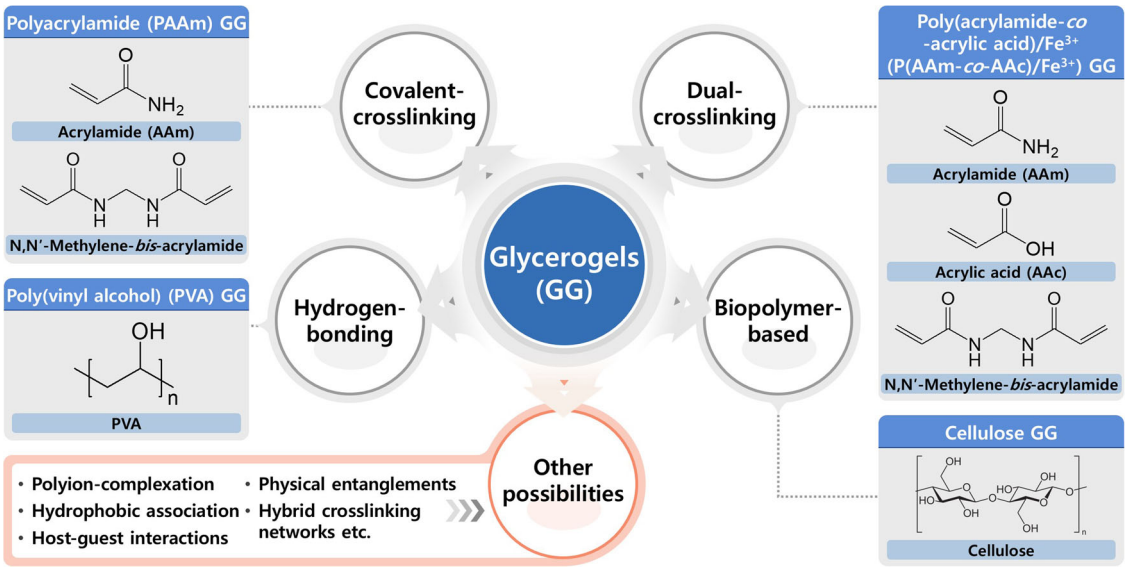

Fig. 2 Different monomers/polymers and crosslinkers used for designing GGs. Method versatility facilitates the design of numerous multifunctional GGs.

a good balance of stiffness (1.6 ± 0.1 MPa), strength (7.1 ± 0.3 MPa), and work of extension (23.5 ± 4.6 MJ m^{-3}) because of the good energy dissipation capability due to its strong ion-coordinated structure. The physically crosslinked cellulose GG exhibits a high stiffness (9.4 ± 0.9 MPa) and strength (2.9 ± 0.1 MPa) and a low stretchability (~100%) due to the highly solvated elongated structure of rigid linear polymers, which have large persistence lengths[7]. By varying the monomer, polymer, and crosslinker compositions, the mechanical properties of each GG developed herein are tunable. In addition, we have evaluated the mechanical stabilities of the GGs at extremely low (−50 °C), room (25 °C), and extremely high (80 °C) temperatures. After prolonged exposure to air (7 d) at −50, 25, or 80 °C, the samples are mounted onto a tensile tester (at room temperature) within 1 min and tested immediately. The mechanical properties of all the GGs remain nearly unchanged (Fig. 3c–f; Fig. S2–S5). We have confirmed that the properties do not change upon exposure for different time periods by testing GG at 1 d, 3 d, and 7 d at 25 °C (Fig. S6). Unlike annealed gels, the mechanical properties of the unannealed sample change with time. More than half of the strength of unannealed PAAm GG is reduced after 7 d of exposure to air at 25 °C (Fig. S7). The annealed sample with a more homogeneous polymer structure remains stable for prolonged periods (Fig. 3). Next, we have investigated the effects of moisture contents on the stabilities of GGs. Because glycerol is known to readily absorb moisture from air, the GGs may keep absorbing moisture under high humidity environments and degrade with time. We have studied the changes in weight and mechanical properties of all four GGs developed herein under prolonged (one week) exposure to high moisture content (~70–90%) (Figs. S8 and S9). The mechanical properties of GGs from swellable polymers—PAAm and P(AAm-co-AAc)—degrade after a significant amount of moisture is absorbed from air. However, interestingly, the nonswellable gels −PVA and cellulose GGs,− which have polymeric chains with crystalline structures[7], do not absorb moisture from air and are not significantly affected by exposure to high moisture. The extreme tolerance of the PAAm and PVA GGs is demonstrated by directly extending and relaxing them at −50 and 80 °C, respectively, inside a chamber after 7 d of exposure (Fig. 3g and h; Movie S1–S4). PAAm GG remains stretchable after 1 month of exposure to extreme temperature (80 °C) (Fig. S10). In sharp contrast to GGs, a PAAm hydrogel completely loses its stretchability within 3 h at −50 and 80 °C and within 1 d at 25 °C (Fig. S11). The brittleness of the PAAm hydrogel at −50 °C is attributed to the formation of ice crystals inside the gel network, whereas at 25 and 80 °C, it is attributed to the complete evaporation of water from the gel network. Furthermore, we have applied a thermal shock of 150 °C for 10 min to the PAAm GG and PAAm hydrogels (Figs. S12 and S13). The GG does not undergo any significant changes in weight and stretchability; however, the hydrogel dries out completely. The high thermal-shock-absorption ability at 150 °C further confirms the durability under harsh conditions induced by the extreme protected network. The scheme for designing extremotolerant GGs is shown in Fig. 2; the proposed method is versatile, such that various functional polymers and crosslinkers are usable for GG fabrication.

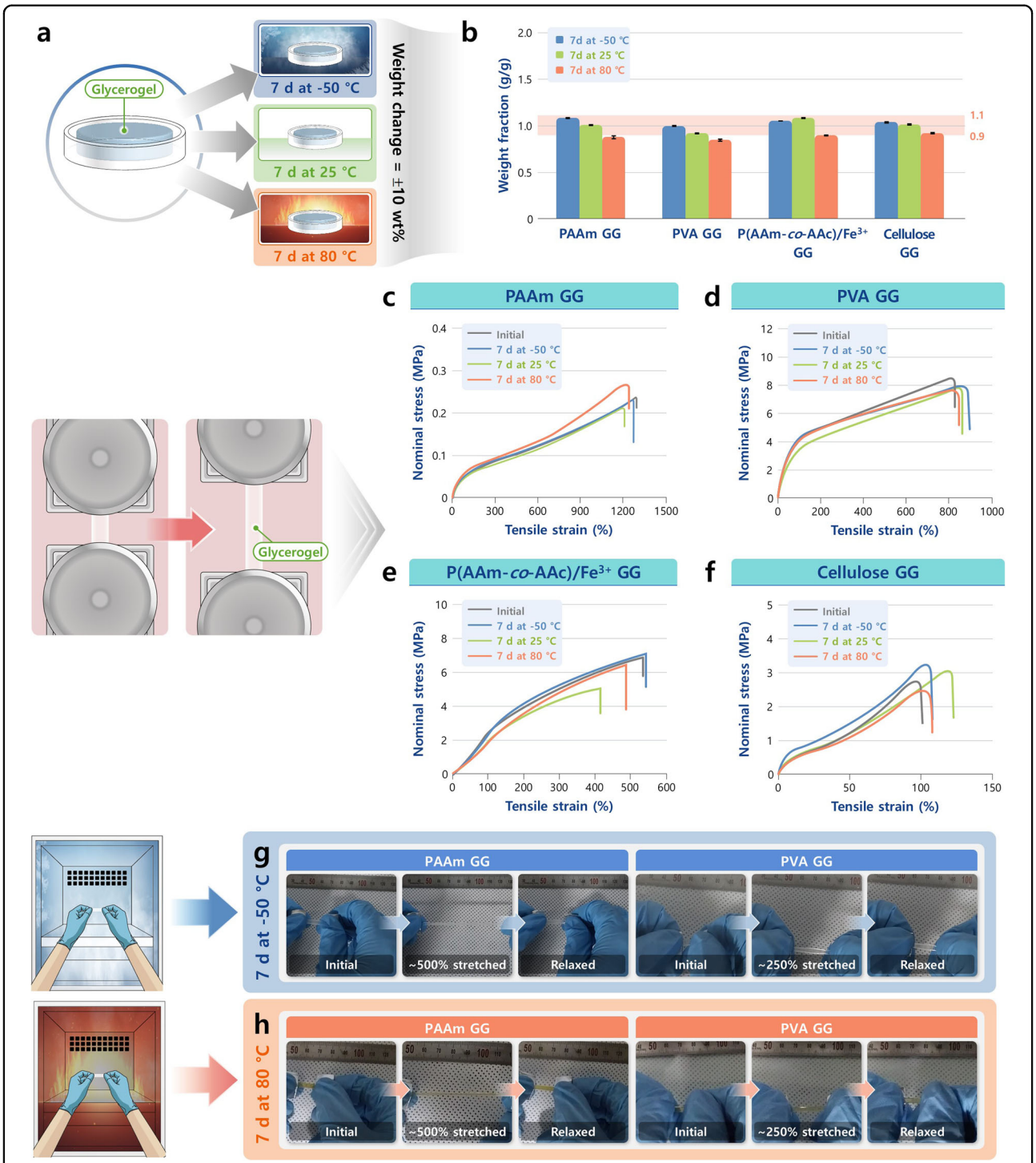

Fig. 3 Characterization of the extremotolerant ability of GGs. a Observation of the effects of low (−50 °C), ambient (25 °C), and high (80 °C) temperatures on the fabricated GGs. **b** Weight fractions of the GGs following incubation for 7 d at −50, 25, and 80 °C. Representative tensile stress–strain curves of (**c**) PAAm, (**d**) PVA, (**e**) P(AAm-*co*-AAc)/Fe^{3+}, and (**f**) cellulose GGs. Tensile tests are performed on pristine samples, and the results are compared with those of the samples incubated at −50, 25, and 80 °C for 7 d. Demonstration of the stretchability of PAAm and PVA GGs following incubation for 7 d at (**g**) −50 °C and (**h**) 80 °C.

We have listed similar types of polyol-based gels available in the literature and compared their mechanical and working temperatures with our GGs (Table S1)[18,19,21,22,25,36]. Our GGs significantly outperform those gels both in mechanical properties and working temperature range. This high performance is attributed to the proposed bioinspired method. As control experiments, we have fabricated PAAm gels directly in various polyol solvents. The results confirm that most polyol solvents are unsuitable for directly fabricating gels with good mechanical integrity due to high-solvent-viscosity- and polymerization-induced phase separation (Fig. S14). Furthermore, we have confirmed that the direct exchange of water in predesigned hydrogels with viscous polyol solvents causes the phase separation of polymers and the notable deswelling of the gels (Fig. S15). This significant difference in swelling suggests facile polymer–solvent interactions by our bioinspired method, preventing aggregation-induced structural collapse and preserving the original structure of the hydrogel (Fig. 1c). Therefore, the solvent contents of our GGs (≥70%) are similar to those of the original hydrogels, and various crosslinking and toughening mechanisms work appropriately for our extremotolerant GGs (Fig. 3c–f; Fig. S15). However, most of the GGs prepared by the direct solvent-exchange strategy are hard, brittle, or plastic-type gels with considerably reduced solvent contents and significantly changed mechanical properties (Figs. S15 and S16). For instance, the tough P(AAm-*co*-AAc)/Fe^{3+} GG fabricated by our method exhibits a tensile strength of 7.1 ± 0.3 MPa and stretchability of 533 ± 76%; the corresponding GG fabricated via direct solvent exchange exhibits brittle, glassy behavior with markedly reduced properties (tensile strength of 1.4 ± 0.4 MPa and stretchability of 14 ± 8%). The extremely high elastic modulus indicates that the GGs fabricated by direct exchange are dominated by glassy structures rather than rubbery polymers. The shrinkage and polymer aggregation of the gel affects its mechanical stability over a wide temperature range. Therefore, the hard, plastic-type PAAm GG (tensile strength of 4.4 MPa) prepared via direct solvent exchange becomes extremely soft (tensile strength of 0.15 MPa) after 3 d of exposure to air at room temperature (Fig. S17).

Notably, the transition from a rubbery to glassy aggregated structure in GGs obtained by the direct exchange method is quite irreversible and cannot be reconfigured by thermal annealing. Therefore, the hard mechanical behaviors of such GGs are not improved after the same thermal treatment as our GGs (Fig. S18). Our comparative studies suggest that the same GGs fabricated by different pathways have dramatic differences in structures and properties. The high swelling and excellent mechanical behaviors of the GGs (low modulus, good strength, high stretchability and work of extension) obtained by our method relative to the direct exchange method clearly indicate that the former method allows smooth solvent replacement; this method provides facile polymer–glycerol interactions and undisturbed polymer conformations without being dramatically aggregated relative to the latter case (Fig. 1c). Because of the preserved structure with well-balanced polymer–solvent interactions, the excellent mechanical properties of our GGs remain stable for a prolonged period over a wide temperature range. The structures and thermal stabilities of the GGs are reconfirmed by DSC analyses (Fig. S19). Both the annealed and unannealed GGs fabricated by our method do not show any thermal transition from −50 to 100 °C, suggesting their extreme tolerance capability. However, the GGs prepared by the direct solvent-exchange strategy show a distinct stepwise endothermic glass transition temperature (T_g), which is between 2 and 55 °C for all the gels studied; therefore, their mechanical performance is hindered over a wide temperature range. These results confirm that the direct solvent exchange of hydrogels with glycerol results in polymer aggregation with glassy transition; with our bioinspired slow-exchange process, this phenomenon is prevented. There is no obvious endothermic transition of water evaporation in the DSC results of our GGs up to 160 °C, apart from the melting transition of PVA crystals, suggesting that there is no notable content of water remaining in the gel network (Fig. S20). Next, we have confirmed the structures of the GGs via SEM. Imaging the GGs using SEM is difficult due to the presence of the solvent. However, after a week of freeze-drying, SEM images of the partially dried P(AAm-*co*-AAc)/Fe^{3+} GGs are obtained; P(AAm-*co*-AAc)/Fe^{3+} GG is chosen because of its relatively low solvent content. The SEM images show a high-density, aggregated polymer structure for the GG fabricated via direct solvent exchange; the corresponding GGs (unannealed and annealed) obtained by our method have a sparse structure, similar to that of the original hydrogel (Fig. S21).

Fracture toughness

The toughness values of the developed GGs are evaluated by tensile fracture tests using notched and unnotched samples (Fig. 4a and b). The fracture energies vary significantly with the polymer and crosslinker types. All the developed GGs exhibit excellent fracture toughness; the PAAm and PVA GGs exhibit the minimum (1325 ± 171 J m^{-2}) and maximum (23053 ± 2284 J m^{-2}) fracture energies, respectively (Fig. 4c). All the GGs exhibit significantly higher fracture toughness than their corresponding hydrogels (Fig. S22). This result suggests that polymers in the glycerol-based microenvironment have higher resistance levels to cracking than those in the water-based microenvironment of hydrogels. Interestingly, the hydroxyl-rich flexible polymer PVA[7] exhibits

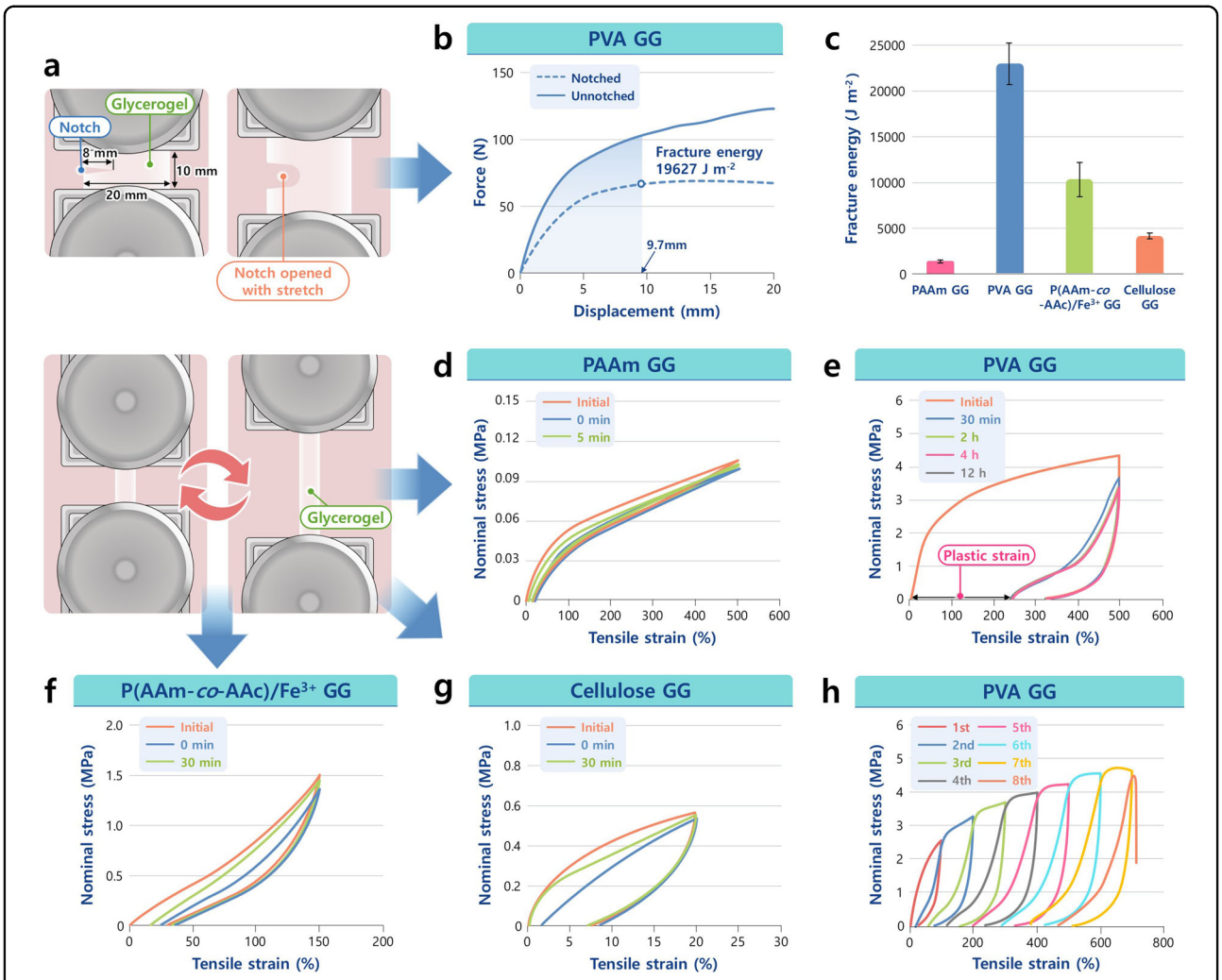

Fig. 4 Fracture toughness, hysteresis, elasticity, and plasticity of the GGs. a Demonstration of the tensile fracture test of the notched sample for the determination of fracture energy. **b** Force vs. displacement curves of the notched and unnotched samples of PVA GG. The critical displacement (L_c) at which cracks begin propagating through the notched sample (detected by video analyses) is identified by the open circle. The fracture energy is determined by dividing the work done (filled area) to stretch the unnotched sample to L_c by the cross-sectional area of the sample. **c** Determined fracture energies of different GGs. Tensile loading–unloading curves of (**d**) PAAm GG, (**e**) PVA GG, (**f**) P(AAm-*co*-AAc)/Fe^{3+}, and (**g**) cellulose GGs at different waiting times. (**h**) Tensile loading–unloading curves of the PVA GG with periodic enhancement in strain by 100% to its fracture point.

the highest enhancement in toughness relative to other gels. Therefore, the increased intermolecular and intramolecular H-bonding networks caused by the three hydroxyl arms of glycerol relative to those caused by the single hydroxyl arm of water are inferred to be the principal contributors to the higher fracture resistance levels of the GGs than those of their corresponding hydrogels. The degree of polymer–solvent H-bonding should be highest for PVA polymer among those of all GGs studied. Consequently, PVA GG have experienced the highest enhancements in toughness relative to those for other gels. The formation of H bonds in GGs is further elucidated by FT–IR measurements (Fig. S23). The stretching vibration of the hydroxyl groups centered at ~3400 cm^{-1} is highly sensitive to H-bonding[42]. The nonbonded hydroxyl groups exhibit an FT–IR peak at >3600 cm^{-1}, and the H-bonded hydroxyl groups exhibit peaks at ≤3400 cm^{-1} depending on the strength of H-bonding[42]. All GGs studied herein exhibit peaks in the range of 3280–3300 cm^{-1}, suggesting that almost all hydroxyl groups are involved in the formation of intermolecular and intramolecular H-bonding networks in the GG systems. Furthermore, among the GGs studied, the hydroxyl-rich flexible polymer-based PVA GG exhibits the lowest wavenumber peak (redshift) at 3281 cm^{-1}, followed by cellulose GG (3291 cm^{-1}), PAAm GG (3293 cm^{-1}), and P(AAm-*co*-AAc)/Fe^{3+} GG (3296 cm^{-1}). These results reconfirm the formation of stronger H bonds in the PVA

GG than in other GGs, which results in the highest enhancement in the fracture toughness of the PVA GG. In addition to polymer–solvent interactions, the dynamic noncovalent bonds between polymers (H bonds, ion-coordination) with an appropriate balance of weak and strong crosslinking points in the P(AAm-*co*-AAc)/Fe^{3+} and PVA GGs induce extreme toughness relative to those of the PAAm and cellulose GGs; this toughness is considerably higher than those of natural rubbers, most biological tissues, and the tough soft materials reported to date[1,2,9–11].

Hysteresis, elasticity, plasticity, and self-recovery

The elasticity, plasticity, energy dissipation, and self-recoverability of GGs are tunable using various crosslinkers and polymers. The covalently crosslinked soft PAAm GG exhibits high nonlinear elasticity with marginal hysteresis despite ~500% loading–unloading (Fig. 4d), which is similar to the PAAm hydrogel[43]. The hysteresis and strength of PAAm GG recover within 5 min of loading–unloading. These results suggest that the PAAm chain in the GG system has dynamics and structure similar to those of the hydrogel system. Unlike PAAm GG, PVA GG exhibits significant hysteresis with a large plastic strain (~250%) at 500% loading–unloading (Fig. 4e). The hysteresis is ~94% of the total work done during 500% loading–unloading, confirming the excellent energy dissipation capability derived from the sacrificial H bonds. The hysteresis and majority of the strain remain unrecovered 12 h after loading–unloading, indicating the plastic deformation of the PVA GG, which is atypical for general hydrogels. The softer PVA GGs (tensile strength <1 MPa), which are prepared with extremely low polymer concentrations (5 and 3 wt.%), exhibit similar plastic behaviors (Fig. S24). PVA GG has marginal hysteresis in the low-strain region (Figure S25), evidencing its good self-recoverability. Following 50 loading–unloading cycles at 10% tension, the hysteresis and strength (~0.65 MPa) of the gel recover completely within 20 min.

The dual-crosslinked P(AAm-*co*-AAc)/Fe^{3+} GG exhibits significant hysteresis at 150% strain, indicating energy dissipation via sacrificial bonds (ion-coordination) (Fig. 4f). Unlike those of PVA GG, most of the hysteresis and strength of P(AAm-*co*-AAc)/Fe^{3+} GG recover within 30 min, suggesting the near-reversibility of the sacrificial bonds. The gel exhibits good recoverability with marginal hysteresis reaching 50% strain, and the recovery times for strength and hysteresis decrease to 5 min (Fig. S26a). The excellent self-recoverability of the gel is further demonstrated by loading the sample at ~50% tension followed by unloading it for 50 cycles (Fig. S26b). Most of the strength and hysteresis of the gel recover within 20 min. The cellulose GG exhibits lower stretchability than other GGs (<150%) because of its high glycerol content (Figure S15) and the rigid nature of the cellulose polymer[7]. However, cellulose GG exhibits significant hysteresis at 20% strain, suggesting efficient energy dissipation by the H bonds in the cellulose network (Fig. 4g). Most of the hysteresis and strength of GG recovered within 30 min, indicating the reversibility of the sacrificial bonds. These results strongly suggest that a wide variety of GGs with tunable elasticity, plasticity, hysteresis, self-recoverability, and fatigue resistance are designable by controlling the polymeric and crosslinked structures.

The excellent plasticity of the PVA GG is studied in depth by applying the repetitive strain of increasing magnitude (Fig. 4h). During cycling, the gel exhibits plastic behavior with accumulated strains. The softer PVA GGs exhibit similar behaviors (Fig. S27). The ratio of the accumulated and applied strains increases significantly with increasing magnitude of applied strain (Fig. S28). High-polymer-density PVA GGs exhibit high accumulated–applied strain ratios. These results suggest that PVA GG possesses tunable plastic behavior. These properties are difficult to achieve in common viscoelastic soft materials. Thus, soft devices with complex 3D configurations or patterned structures can be fabricated via plastically deformed bending/twisting/rolling/patterning.

The mechanical properties of all the GGs are tuned by the judicious variations in polymers and crosslinkers. At low energy dissipation, GG with a soft polymer (PAAm) with loose covalently crosslinked structures possesses high stretchability and self-recoverability. Extremely high toughness, stretchability, and strength of the PVA GGs are achieved because of the efficient energy dissipation facilitated by high-density sacrificial H bonds in soft PVA polymers. In PVA GGs, plastic deformation causes large irreversible hysteresis. The efficient and reversible energy dissipation of dual-crosslinked (covalent and ion-coordinated) GGs imparts a balance of softness, strength, and toughness while inducing excellent self-recoverability and low hysteresis. H-bond-based GGs fabricated from rigid natural polymers (such as cellulose) have lower stretchability than soft PVA GGs and show excellent stiffness, strength, and toughness due to their efficient energy dissipation. The mechanical properties of rigid natural polymers can be tuned extensively by integrating our recent method to create various biomimetic superstructures[1,6–8]. The results of this study suggest that a wide variety of properties and functions are induced in extremotolerant GGs by exploiting their rich hydrogel chemistry.

Self-weldability

The versatile applicability of the GGs is further extended by their excellent self-welding capabilities. A self-welding method is developed for efficiently joining cellulose-based hydrogels via ion-induced polymer

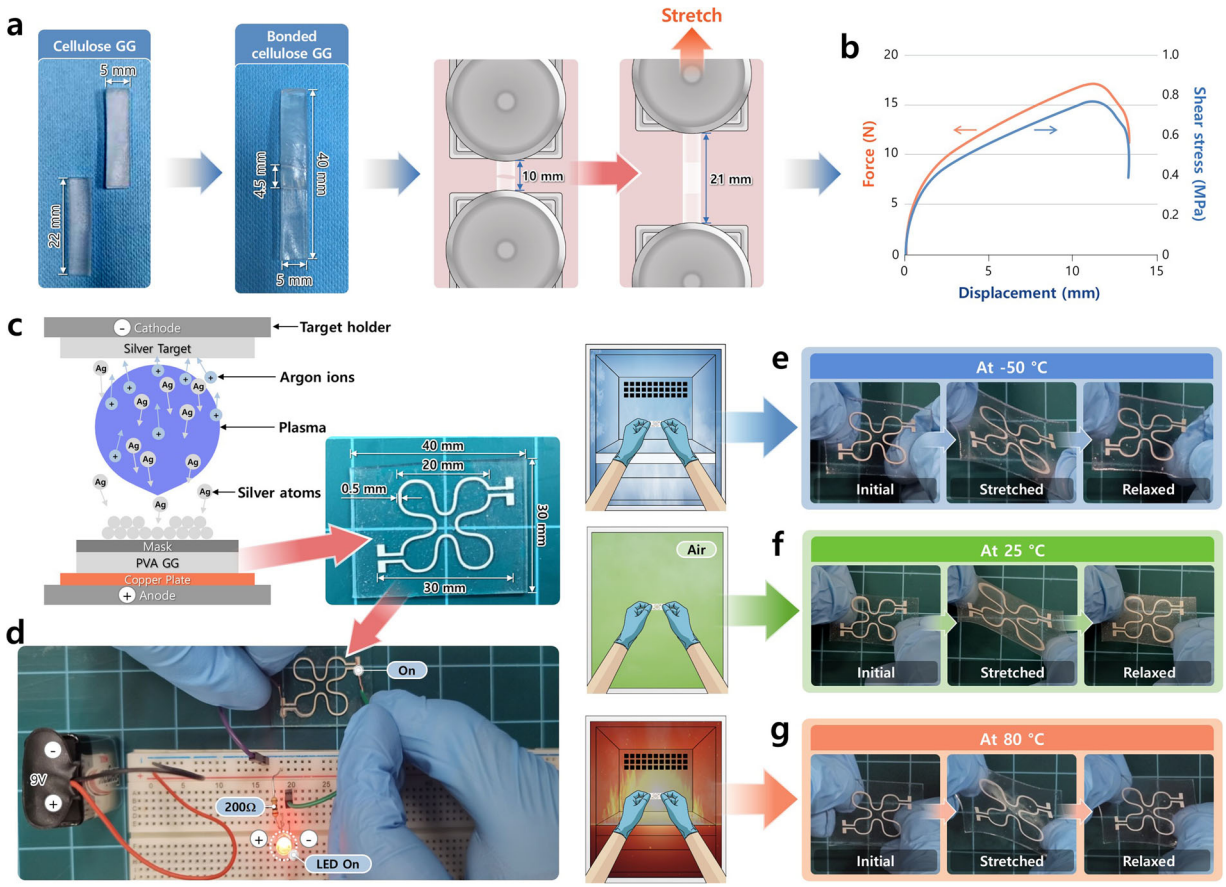

Fig. 5 GG-based self-welding and stretchable electrical pattern. a Demonstration of the self-welding process of cellulose GG. **b** Lap shear test result to determine the shear adhesive force and strength of the welded cellulose GG. **c** Illustration and photograph of the silver-patterned PVA GG fabricated by the mask-controlled ion-sputtering process. **d** LED switching by the patterned PVA GG connected to a 9 V battery with a 200 Ω resistor. **e**–**g** Demonstration of the stretchability of the patterned PVA GG at −50, 25, and 80 °C.

reconfiguration[8], which is applied to physically crosslinked GG systems. The welding efficiency is quantitatively determined by performing the lap shear test on coaxially joined GGs (Fig. 5a and b). The welded cellulose GG exhibits an adhesive strength of 0.77 MPa, which is markedly higher than those of adhesive hydrogels and similar to those of cartilage–bone or hydrogel–bone bonds[8]. Furthermore, the welded sample stretches >100%, demonstrating excellent bonding toughness. Similar to cellulose GG, welded soft PVA GG (fabricated from a 5 wt.% PVA precursor) exhibit good adhesive strength (0.21 MPa) (Fig. S29). Physically crosslinked GGs exhibit excellent self-welding capabilities imparted by ion-induced structural reconfiguration, creating a significant advantage when designing various extremotolerant devices with complex 3D structures.

Electrical patternability

Various tailored functionalized GGs have demonstrated their potential for diverse next-generation electrical/electronic applications. Electrically conductive GGs have been prepared by coating silver onto GGs via high-speed ion-sputtering[44]. By using a predesigned mask (Fig. S30), a thin layer of a simple fractal-designed[45] silver pattern loop has been created flawlessly on a soft PVA GG (Fig. 5c). Facile lighting of a light-emitting diode (LED) using the patterned GG suggests that the silver pattern is well-connected at a microscopic level and completes the circuit (Fig. 5d; Movie S5). The stability and stretchability of the patterned GG are demonstrated at −50, 25, and 80 °C (Fig. 5e–g; Movies S6–S8), at which point the gel stretches and recovers almost completely undamaged, confirming the formation of a highly stable pattern. In general, metal deposition on soft materials is difficult because high-speed ion sputtering generates considerable heat around the sputtering region. The structural and thermal stabilities of the GGs and good polymer–silver particle adhesion induce the stretchability of the hybrid GG from −50 to 80 °C without any interfacial failure.

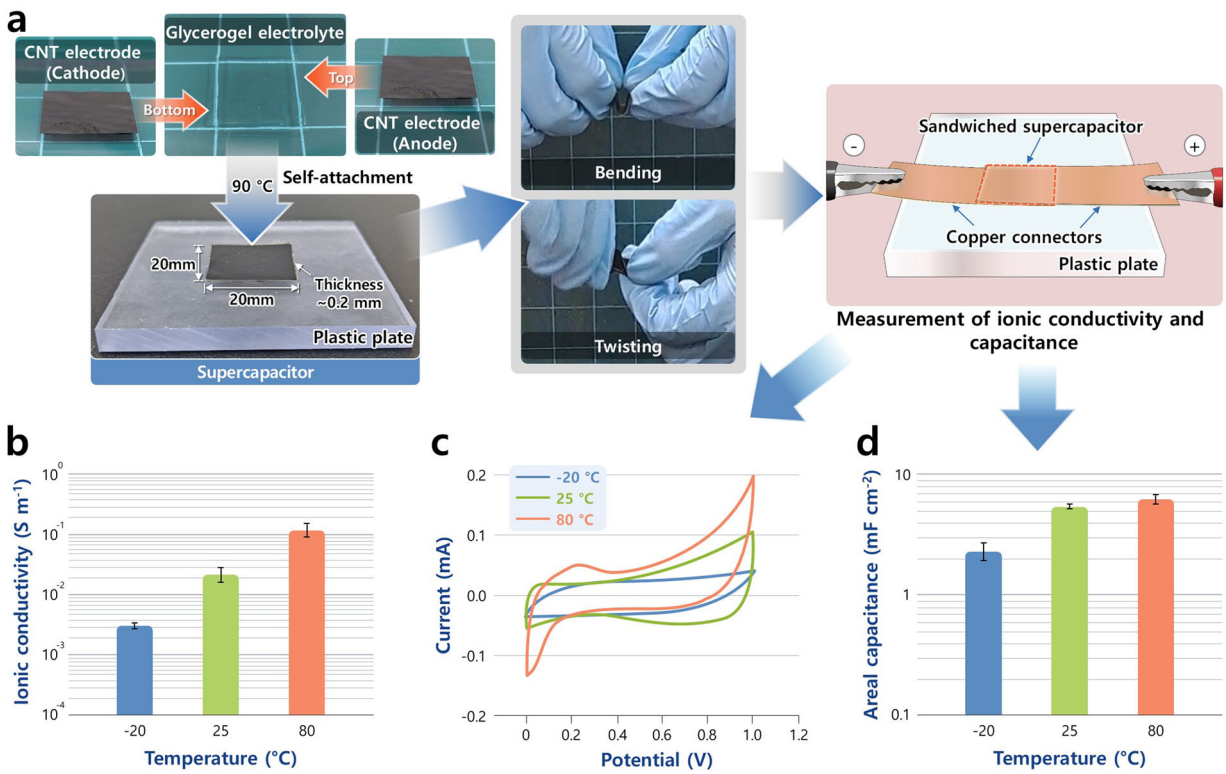

Fig. 6 GG-based flexible electrolyte and supercapacitor. a Fabrication and characterization of the flexible PVA-GG-electrolyte-based supercapacitor. **b** Ionic conductivities of the PVA GG electrolyte at different temperatures. **c** Cyclic voltammograms recorded at a scan rate of 1 mV s^{-1}. **d** Calculated areal capacitance of the supercapacitor device measured at different temperatures.

GG-based electrolyte and supercapacitor

Furthermore, ionically conductive GGs are developed. Glycerol readily dissolves numerous common inorganic salts because of its hydrophilicity and polarity. For instance, $LiClO_4$ is widely used in preparing battery and supercapacitor electrolytes[46,47] and is soluble in glycerol at high concentrations. As an example, $LiClO_4$-ion-loaded PVA GG electrolytes are prepared by simple diffusion-induced ion loading[47]. Thereafter, a prototype supercapacitor is fabricated by sandwiching the as-prepared PVA GG electrolyte sheet (~0.2 mm thick) between two CNT-based flexible electrode films. The subsequent annealing step induces strong electrode–gel surface self-attachment, imparting excellent mechanical stability to the device. Consequently, the device exhibits high flexibility upon bending and twisting with no interfacial failure (Fig. 6a; Movie S9). The PVA GG electrolyte exhibits an ionic conductivity of 0.021 ± 0.006 S m^{-1} at 25 °C. The conductivity decreases and increases with decreases and increases in the temperature, respectively (Fig. 6b, Fig. S31), which is attributed to the change in the solvent viscosity with temperature. GG attains a high conductivity of 0.11 ± 0.03 S m^{-1} at 80 °C and maintains a conductivity of 0.003 ± 0.0003 S m^{-1} at −20 °C, which is similar to that of gel electrolytes used for energy-storage devices[18,47,48].

The supercapacitor exhibits a quasirectangular closed loop in the CV, suggesting ideal electric double-layer capacitor (EDLC) behavior. Even at high scan rates, the device exhibits similar CV profiles within the 0–1 V voltage window (Figure S32). The GCD curves exhibit a symmetric triangular shape at different current rates, confirming ideal EDLC behavior (Figure S33). The areal capacitance is calculated as 5.29 ± 0.24 mF cm^{-2} at 1 mV s^{-1} (CV curve) and 7.46 ± 0.63 mF cm^{-2} at 0.1 mA (GCD curve). The areal capacitance obtained from the CV and GCD curves remains constant with the scan rate and current density variations. Furthermore, the device exhibits excellent performance from −20 to 80 °C (Fig. 6c and d). The CV curves show closed quasirectangular loops. The areal capacitances of the device are 5.97 ± 0.49 and 2.21 ± 0.36 mF cm^{-2} at 80 and −20 °C, respectively. These values are very similar to those obtained from GCD (Fig. S34) and to those of several high-performance supercapacitors (Fig. S35). The change in the areal capacitance with temperature closely resembles the change in the ionic conductivity of the GG electrolyte at the

corresponding temperatures. The excellent ion solvation and extremoresistance of glycerol induce good ion-conduction pathways in the GG-based electrolyte, resulting in good capacitance over a wide temperature range.

Conclusions

In summary, a novel class of extremotolerant GGs with wide-ranging tailored properties and functionalities was developed using a very slow but simple two-step structure-forming technique, which mimicked tun formation in tardigrades. Initially, the water-to-glycerol solvent exchange of the predesigned hydrogels was performed step-by-step at room temperature for the water-stable equilibrated hydrogels (PVA, cellulose, and P(AAm-*co*-AAc)/Fe^{3+}) and directly at high temperatures for the water-swellable as-prepared hydrogel (PAAm). Thereafter, the as-prepared gels were thermally annealed to relieve undesired residual stress on the gel network and to uniformly distribute the polymers and crosslinking structures. This versatile, bioinspired method allowed glycerol tolerance to a wide range of temperatures to form an extreme protected network via intramolecular and intermolecular H bonding with various hydrophilic polymers. The method facilitated the creation of a suitable microenvironment for the formation of various crosslinking structures, the realization of toughening mechanisms, and the integration with various functional materials, thus paving the way for diverse functionalization. The stiffness, strength, toughness, elasticity, plasticity, and self-recoverability were judiciously tuned by varying the polymers and crosslinking structures. Irrespective of their internal chemistry, the GGs demonstrated long-term stability from −50 to 80 °C with a thermal-shock-absorption ability at 150 °C; this value had not yet been achieved in gel materials to the best of our knowledge. A self-weldable GG, stretchable and metal-patterned electrically conductive GG, ionically conductive GG, and prototype GG-based flexible supercapacitor with excellent capacitance were developed to demonstrate their potential for many next-generation applications, including extremotolerant energy-storage devices, sensors or actuators, and soft robotics systems. This study facilitated the rational design of a wide range of extremotolerant GGs to satisfy the stringent fabrication requirements of next-generation devices by harnessing available hydrogels that have wide-ranging functionalities and properties to date.

Acknowledgements
This work was supported by National Research Foundation of Korea (NRF) grants funded by the Korean government (MSIT) [grant numbers 2020R1A2C2007974, 2021R1A4A1029780]. Md.T.I.M. acknowledges the financial support from the Brain Pool program through the NRF funded by the MSIT [grant number 2019H1D3A1A02070510].

Author contributions
Md.T.I.M. and I.J. conceived and designed the study. Md.T.I.M., Y.L., A.V.R.V., T.G., and R.R.M.W. performed the experiments. All the authors discussed the results and contributed to data interpretation. Md.T.I.M. and I.J. wrote the manuscript.

Conflict of interest
The authors declare no competing interests.

Supplementary information The online version contains supplementary material available at https://doi.org/10.1038/s41427-023-00472-1.

Received: 2 January 2023 Revised: 17 February 2023 Accepted: 24 February 2023.
Published online: 7 April 2023

References

1. Mredha, Md. T. I. & Jeon, I. Biomimetic anisotropic hydrogels: advanced fabrication strategies, extraordinary functionalities, and broad applications. *Prog. Mater. Sci.* **124**, 100870 (2022).
2. Mredha, Md. T. I., Pathak, S. K., Tran, V. T., Cui, J. & Jeon, I. Hydrogels with superior mechanical properties from the synergistic effect in hydrophobic–hydrophilic copolymers. *Chem. Eng. J.* **362**, 325–338 (2019).
3. Cianchetti, M., Laschi, C., Menciassi, A. & Dario, P. Biomedical applications of soft robotics. *Nat. Rev. Mater.* **3**, 143–153 (2018).
4. Hao, X. P. et al. Kirigami-design-enabled hydrogel multimorphs with application as a multistate switch. *Adv. Mater.* **32**, 2000781 (2020).
5. Jeon, I., Cui, J., Illeperuma, W. R. K., Aizenberg, J. & Vlassak, J. J. Extremely stretchable and fast self-healing hydrogels. *Adv. Mater.* **28**, 4678–4683 (2016).
6. Tran, V. T. et al. Electrically, thermally, and mechanically anisotropic gels with a wide operational temperature range. *Adv. Funct. Mater.* **32**, 2110177 (2022).
7. Mredha, Md. T. I. et al. A facile method to fabricate anisotropic hydrogels with perfectly aligned hierarchical fibrous structures. *Adv. Mater.* **30**, 1704937 (2018).
8. Mredha, Md. T. I. et al. Anisotropic tough multilayer hydrogels with programmable orientation. *Mater. Horiz.* **6**, 1504–1511 (2019).
9. Gong, J. P., Katsuyama, Y., Kurokawa, T. & Osada, Y. Double-network hydrogels with extremely high mechanical strength. *Adv. Mater.* **15**, 1155–1158 (2003).
10. Sun, J.-Y. et al. Highly stretchable and tough hydrogels. *Nature* **489**, 133–136 (2012).
11. Furukawa, H. et al. Tear velocity dependence of high-strength double network gels in comparison with fast and slow relaxation modes observed by scanning microscopic light scattering. *Macromolecules* **41**, 7173–7178 (2008).
12. Mredha, Md. T. I., Le, H. H., Cui, J. & Jeon, I. Double-hydrophobic-coating through quenching for hydrogels with strong resistance to both drying and swelling. *Adv. Sci.* **7**, 1903145 (2020).
13. Jian, Y. et al. Biomimetic anti-freezing polymeric hydrogels: keeping soft-wet materials active in cold environments. *Mater. Horiz.* **8**, 351–369 (2021).
14. Niu, Y. et al. The new generation of soft and wearable electronics for health monitoring in varying environment: From normal to extreme conditions. *Mater. Today* **41**, 219–242 (2020).
15. Niu, C., An, L. & Zhang, H. Mechanically robust, antifatigue, and temperature-tolerant nanocomposite ionogels enabled by hydrogen bonding as wearable sensors. *ACS Appl. Polym. Mater.* **4**, 4189–4198 (2022).
16. Cho, C.-W., Pham, T. P. T., Zhao, Y., Stolte, S. & Yun, Y.-S. Review of the toxic effect of the ionic liquids. *Sci. Total Environ.* **786**, 147309 (2021).
17. Liu, J. et al. Metallopolymer organohydrogels with photo-controlled coordination crosslinks work properly below 0 °C. *Adv. Mater.* **32**, 1908324 (2020).
18. Rong, Q., Lei, W., Huang, J. & Liu, M. Low temperature tolerant organohydrogel electrolytes for flexible solid-state supercapacitors. *Adv. Energy Mater.* **8**, 1801967 (2018).

19. Rong, Q. et al. Anti-freezing, conductive self-healing organohydrogels with stable strain-sensitivity at subzero temperatures. *Angew. Chem. Int. Ed. Engl.* **56**, 14159–14163 (2017).
20. Chen, F. et al. Rational fabrication of anti-freezing, non-drying tough organohydrogels by one-pot solvent displacement. *Angew. Chem. Int. Ed. Engl.* **57**, 6568–6571 (2018).
21. Ju, M., Wu, B., Sun, S. & Wu, P. Redox-active iron-citrate complex regulated robust coating-free hydrogel microfiber net with high environmental tolerance and sensitivity. *Adv. Funct. Mater.* **30**, 1910387 (2020).
22. Chen, M. et al. Anti-freezing flexible aqueous Zn–MnO_2 batteries working at −35 °C enabled by a borax-crosslinked polyvinyl alcohol/glycerol gel electrolyte. *J. Mater. Chem. A* **8**, 6828–6841 (2020).
23. Guo, M. et al. A highly stretchable, ultra-tough, remarkably tolerant, and robust self-healing glycerol-hydrogel for a dual-responsive soft actuator. *J. Mater. Chem. A* **7**, 25969–25977 (2019).
24. Han, L. et al. Mussel-inspired adhesive and conductive hydrogel with long-lasting moisture and extreme temperature tolerance. *Adv. Funct. Mater.* **28**, 1704195 (2018).
25. Seo, Y. et al. Transparent and flexible electronics assembled with metallic nanowire-layered nondrying glycerogel. *ACS Appl. Mater. Interfaces* **12**, 13040–13050 (2020).
26. Li, C., Deng, X. & Zhou, X. Synthesis antifreezing and antidehydration organohydrogels: one-step in-situ gelling versus two-step solvent displacement. *Polymers* **12**, 2670 (2020).
27. Lee, J. et al. Water-processable, stretchable, self-healable, thermally stable, and transparent ionic conductors for actuators and sensors. *Adv. Mater.* **32**, 1906679 (2020).
28. Sato, K. et al. Phase-separation-induced anomalous stiffening, toughening, and self-healing of polyacrylamide gels. *Adv. Mater.* **27**, 6990–6998 (2015).
29. Tsujimoto, M., Imura, S. & Kanda, H. Recovery and reproduction of an Antarctic tardigrade retrieved from a moss sample frozen for over 30 years. *Cryobiology* **72**, 78–81 (2016).
30. Crowe, J. H. & Crowe, L. M. Preservation of mammalian cells—learning nature's tricks. *Nat. Biotechnol.* **18**, 145–146 (2000).
31. Bertolani, R. et al. Experiences with dormancy in tardigrades. *J. Limnol.* **63**, 16–25 (2004).
32. Somme, L. Anhydrobiosis and cold tolerance in tardigrades. *Eur. J. Entomol.* **93**, 349–357 (1996).
33. Tudorache, M., Negoi, A., Tudora, B. & Parvulescu, V. I. Environmental-friendly strategy for biocatalytic conversion of waste glycerol to glycerol carbonate. *Appl. Catal., B* **146**, 274–278 (2014).
34. Basiak, E., Lenart, A. & Debeaufort, F. How glycerol and water contents affect the structural and functional properties of starch-based edible films. *Polymers* **10**, 412 (2018).
35. Gu, Y. & Jérôme, F. Glycerol as a sustainable solvent for green chemistry. *Green. Chem.* **12**, 1127–1138 (2010).
36. Zha, X.-J. et al. Nanofibrillar poly(vinyl alcohol) ionic organohydrogels for smart contact lens and human-interactive sensing. *ACS Appl. Mater. Interfaces* **12**, 23514–23522 (2020).
37. Zondervan, R., Kulzer, F., Berkhout, G. C. G. & Orrit, M. Local viscosity of supercooled glycerol near T_g probed by rotational diffusion of ensembles and single dye molecules. *Proc. Natl. Acad. Sci. U. S. A.* **104**, 12628–12633 (2007).
38. Wu, M., Chen, X., Xu, J. & Zhang, H. Freeze-thaw and solvent-exchange strategy to generate physically cross-linked organogels and hydrogels of curdlan with tunable mechanical properties. *Carbohydr. Polym.* **278**, 119003 (2022).
39. Xu, L. et al. A solvent-exchange strategy to regulate noncovalent interactions for strong and antiswelling hydrogels. *Adv. Mater.* **32**, 2004579 (2020).
40. Prameela, S. E. et al. Materials for extreme environments. *Nat. Rev. Mater.* **8**, 81–88 (2023).
41. Trieu, H. & Qutubuddin, S. Poly(vinyl alcohol) hydrogels: 2. Effects of processing parameters on structure and properties. *Polymer* **36**, 2531–2539 (1995).
42. Nam, C., Zimudzi, T. J., Geise, G. M. & Hickner, M. A. Increased hydrogel swelling induced by absorption of small molecules. *ACS Appl. Mater. Interfaces* **8**, 14263–14270 (2016).
43. Kim, J., Zhang, G., Shi, M. & Suo, Z. Fracture, fatigue, and friction of polymers in which entanglements greatly outnumber cross-links. *Science* **374**, 212–216 (2021).
44. Hu, Z., Chen, Y., Wang, C., Zheng, Y. & Li, Y. Polymer gels with engineered environmentally responsive surface patterns. *Nature* **393**, 149–152 (1998).
45. Fan, J. A. et al. Fractal design concepts for stretchable electronics. *Nat. Commun.* **5**, 3266 (2014).
46. Younesi, R., Veith, G. M., Johansson, P., Edström, K. & Vegge, T. Lithium salts for advanced lithium batteries: Li–metal, Li–O_2, and Li–S. *Energy Environ. Sci.* **8**, 1905–1922 (2015).
47. Lu, N. et al. Rational design of antifreezing organohydrogel electrolytes for flexible supercapacitors. *ACS Appl. Energy Mater.* **3**, 1944–1951 (2020).
48. Li, X. et al. Flexible supercapacitor based on organohydrogel electrolyte with long-term anti-freezing and anti-drying property. *Adv. Funct. Mater.* **30**, 2007291 (2020).